

Original Article

Intravoxel incoherent motion diffusion weighted imaging of high-grade gliomas and brain metastases: efficacy in preoperative differentiation

Shuangshuang Song, Jiping Zhao, Pining Zhang, Huawei Su, Qinglan Sui, Xiaoming Zhou, Xuejun Liu, Lei Niu

Department of Radiology, The Affiliated Hospital of Qingdao University, Qingdao, China

Received September 5, 2017; Accepted April 2, 2018; Epub July 15, 2018; Published July 30, 2018

Abstract: *Background and purpose:* High-grade gliomas and metastatic tumors are two most common malignant brain tumors worldwide, but the treatments are completely different. Therefore, confirming the nature of the tumor prior to surgery is critically important for guiding clinical treatment. Traditionally apparent diffusion coefficient (ADC) values of diffusion weighted imaging (DWI) are used to assess the microscopic displacement of water molecules inside the tumor, while, it can also be affected by pseudorandom motion caused by microcapillary, so, the reliability of the tumor diagnosis attained through traditionally ADC is questioned. Intravoxel incoherent motion imaging diffusion weighted imaging (IVIM-DWI) can quantify both diffusion and perfusion values respectively through a biexponential model. This study therefore aimed to investigate the application of related parameters about diffusion and perfusion of IVIM-DWI for the differential diagnosis of high-grade gliomas and metastatic tumors. *Methods:* Twenty-four cases of high-grade gliomas and 28 cases of metastatic tumors were confirmed pathologically. We retrospectively reviewed the data of conventional MRI and IVIM-DWI prior to any treatment, to separately measure the D value, D* value and f in tumor parenchyma, peritumoral edema (within 1 cm), and centrum semiovale on the contralateral and calculate the relative parameters. Different parameters were statistically analyzed using an independent samples t-test and receiver operating characteristics (ROC) curves. *Results:* D*, rD* values obtained from the tumor parenchyma and peritumoral edema of high-grade gliomas were both higher than metastatic tumors (P<0.05), f values and rf values were both lower than metastatic tumors (P<0.01). ROC curves showed the parameters with statistical significance were valuable to a certain extent in the clinical diagnoses. D and rD values were not statistically different in the tumor parenchyma and peritumoral edema (within 1 cm) of high-grade gliomas and metastatic tumors (P>0.05). Statistical analysis showed that statistical differences in D, D*, f, and rD*, rD, rf values were consistent between the two types of tumors. *Conclusion:* IVIM-DWI can differentiate the diffusion and perfusion between high-grade gliomas and brain metastases, either in the tumor parenchyma or in the peritumoral edema, providing important application values in the differential diagnosis of high-grade gliomas and metastatic tumors.

Keywords: Multi-b value, IVIM, ADC, high-grade gliomas, metastatic tumors

Introduction

With the development of imaging technology, a variety of functional imaging techniques of magnetic resonance imaging such as diffusion-weighted imaging (DWI), diffusion tensor imaging (DTI), dynamic contrast enhancement (DCE), perfusion weighted imaging (PWI), hydrogen proton magnetic resonance spectroscopy (MRS), arterial spin labelling (ASL) have consequently been developed. From morphology to quantitative function, and from macro developments to microscopic molecular levels, abundant infor-

mation has been provided for the identification of high-grade gliomas and metastatic tumors. Intravoxel incoherent motion (IVIM) uses multiple b-value diffusion weighted imaging (DWI) for quantitative analysis of water molecules diffusion and microcirculation perfusion of two kinds of moving components, and supplying simple and reliable evidence for correct diagnosis.

In the 1980s, Le Bihan et al [1, 2] suggested the use of IVIM to describe microscopic intravoxel activity, theorizing that blood circulation and perfusion are non-uniform, unorganized

Differentiation of high-grade gliomas and brain metastases by IVIM-DWI

random activity, and that capillary circulation and molecular diffusion both will have equally effects on signal strength under low b-value conditions, and signal strength will attenuate in a double exponential manner. The IVIM-DWI technique can not only evaluate molecular diffusion of water, but also reflect capillary perfusion conditions. D^* (also called fast ADC) can be defined as the pseudo-diffusion coefficient which macroscopically describes the incoherent motion of blood within the capillary network, f (also called the fraction of fast ADC) indicates the fraction of perfusion-related signal decay over the total incoherent diffusion signal decay within each voxel [3], and D (also called slow ADC) as the true molecular diffusion coefficient.

Through IVIM-DWI, we measured the perfusion coefficient D^* , diffusion coefficient D , and perfusion fraction f separately in tumor parenchyma, peritumoral edema (within 1 cm), and centrum semiovale on the contralateral of high-grade gliomas and metastatic tumors. Parameters were analyzed to determine the statistical differences and investigate the diffusion and perfusion states in different parts of the two tumors, and provide precise information for the identification. In this study, we also calculated relative values of D , D^* , and f respectively, i.e. rD^* , rD , and rf , to eliminate individual differences, and to increase objectivity and realistically of revealing differences between the two tumors.

Materials and methods

Patient population

The Institutional Review Board of the Affiliated Hospital of Qingdao University approved this retrospective study and waived the need for written informed consent from the participants. Between June 2016 and July 2017, MRI scans were performed in our hospital on 24 cases of high-grade gliomas (WHO grade III, $n=8$; WHO grade IV, $n=16$), 17 were male and 7 were female. The overall median age was 57 years (range, 32-80 years); 28 cases of metastatic tumors (primary tumor: lung cancer, $n=21$; esophageal cancer, $n=3$; rectal cancer, $n=4$), 10 were male and 18 were female. The overall median age was 54 years (range, 31-77 years). All patients were included on the basis of the

following criteria: (a) MRI scan, IVIM-DWI and MRI enhancement scan were performed at the same time prior to any treatment; (b) high-grade gliomas ($n=24$), primary tumors of the metastasis and the brain metastases ($n=28$) were confirmed by surgery and pathology; (c) no significant motion-related artifact. Patients with recurrent tumors were excluded and none of the included patients had neurological disorders other than high-grade gliomas or brain metastases. (d) the minimum length of edema around every lesions was more than 1 cm.

MRI acquisition protocols

This study was performed on a 3 Tesla (T) MRI machine (Signa; GE; Milwaukee, WI, U.S.A.) equipped with an eight-channel sensitivity encoding head coil. The order of our brain tumor imaging protocol was as follows: T1 FLAIR, FSE T2-weighted imaging, T2 FLAIR, DWI, IVIM MR imaging, and contrast-enhanced T1 FLAIR.

T1 FLAIR was obtained with the following parameters: repetition time (TR)/echo time (TE)/ inversion time (TI), 2500/24/860 ms; the TR/TE of FSE T2-weighted imaging were 4320/120 ms; the TR/TE/TI of T2 FLAIR were 8000/165/2100 ms; DWI was acquired in three orthogonal directions, combined into a trace image and with the following parameters: TR/TE, 5500/73.9 ms; diffusion gradient encoding, $b=0$, 1000 s/mm². They were obtained with the following parameters: field of view (FOV), 24 cm; number of excitations (NEX) was 1, slice thickness/gap, 5 mm/1.5 mm; matrix, 512×512.

For the IVIM MR imaging, thirteen different b-values were acquired (20, 40, 60, 80,100, 150, 200, 400, 600, 800, 1000, 1200 and 1500 s/mm²) in three orthogonal directions and the corresponding traces were calculated prior to contrast injection. The imaging parameters for IVIM were as follows: TR/TE, 6075/81.5 ms; a slice thickness, 5 mm; NEX was 2; and a matrix number, 160×160, and the total acquisition time for IVIM was 8 min 12 seconds.

After the scan of conventional MR imaging, contrast T1 FLAIR of sagittal, axial and coronal images were acquired. Gadolinium-diethylene triamine pentaacetic acid (Gd-DTPA) was intravenously injected at a dose of 0.1 mmol/kg and

Differentiation of high-grade gliomas and brain metastases by IVIM-DWI

Table 1. Comparison of parameters in tumor parenchyma of high-grade gliomas and metastatic tumors

Parameters	High-grade gliomas	Metastatic tumors	t-value	P-value
D* ($\times 10^{-3}$ mm ² /s)	5.52 \pm 1.12	4.28 \pm 1.46	-2.927	0.006
rD* ($\times 100\%$)	2.32 \pm 0.94	1.70 \pm 0.63	-2.449	0.019
D ($\times 10^{-4}$ mm ² /s)	8.01 \pm 1.43	8.06 \pm 2.16	0.080	0.937
rD ($\times 100\%$)	1.22 \pm 0.32	1.24 \pm 0.34	0.206	0.838
f (%)	19.73 \pm 4.25	30.30 \pm 12.20	3.494	0.001
rf ($\times 100\%$)	1.39 \pm 0.43	2.11 \pm 0.89	3.169	0.003

Data were showed as mean \pm SD.

at a rate of 5 mL/s. The imaging parameters for contrast T1 FLAIR were the same with T1 FLAIR.

Image analyses and quantification of imaging parameters

Original IVIM-DWI images were transferred to an AW4.6 postprocessing workstation of GE. Using MADC software, data was post-processed and a pcolor map was produced with corresponding parameters. Using conventional MR images as a reference, the tumor parenchyma, peritumoral edema within 1 cm and the contralateral centrum semiovale were selected as regions of interest (ROI), while blood vessels, cystic degenerations, necrosis and regions with hemorrhage were excluded. Three ROIs were selected from each area, and the mean value of D*, D, and f values were obtained. Parameter values of tumor parenchyma and peritumoral edema within 1 cm of high-grade gliomas and metastatic tumors were divided by the corresponding values of contralateral centrum semiovale to obtain relative values, such as: $rD^*_{\text{tumor parenchyma}} = D^*_{\text{tumor parenchyma}} / D^*_{\text{contralateral centrum semiovale}}$

Statistical analyses

A normal distribution of the data was assumed. All data are expressed as mean \pm standard deviation (SD). Different parameters in the corresponding regions of high-grade gliomas and metastatic tumors were statistically analyzed using an independent samples t-test. Receiver operating characteristics (ROC) curve was employed to analyze the parameter's statistical difference to determine the optimal threshold, the sensitivity and the specificity. SPSS 20.0 for Windows (SPSS, Chicago, IL, USA) was used to perform all statistical analyses; $p < 0.05$ indicated statistical significance.

Results

Comparisons of the parameters in tumor parenchyma, peritumoral edema within 1 cm of high-grade gliomas and metastatic tumors

D* and rD* values obtained from the tumor parenchyma of high-grade gliomas were both higher than those of the metastatic tumors ($P < 0.05$),

f and rf values obtained from the tumor parenchyma of high-grade gliomas were both lower than those of the metastatic tumors ($P < 0.01$). D and rD values were not statistically different in the tumor parenchyma of high-grade gliomas and metastatic tumors ($P > 0.05$, **Table 1** and **Figures 1, 2**).

D* and rD* values obtained from peritumoral edema within 1 cm of high-grade gliomas were both higher than those of the metastatic tumors ($P < 0.05$), while f and rf values were both lower than those of the metastatic tumors ($P < 0.01$). But D and rD values were not statistically different in peritumoral edema within 1 cm of high-grade gliomas and metastatic tumors ($P > 0.05$, **Table 2** and **Figures 1, 2**).

Statistical analysis showed that statistical differences in D, D*, f, and rD*, rD, rf values were consistent between the two tumors, so, our discussion in the following will only focused on the D, D*, and f values.

ROC curve analysis of the parameters with statistical difference

Table 3 and **Figure 3** showed that D*, rD*, f, and rf values were valuable to a certain extent in clinical diagnoses, among which the D* values from the peritumoral edema (AUC=0.910, $P < 0.001$, sensitivity 100%, uniqueness 100%) was even more useful in diagnoses, with a suggested threshold value of 3.19×10^{-3} mm²/s.

Discussion

In this study, we found that D* values obtained from the tumor parenchyma of high-grade gliomas (5.52 \pm 1.12) were higher than that of metastatic tumors (4.28 \pm 1.46), with a statistically significant difference ($P = 0.006$), indicating that

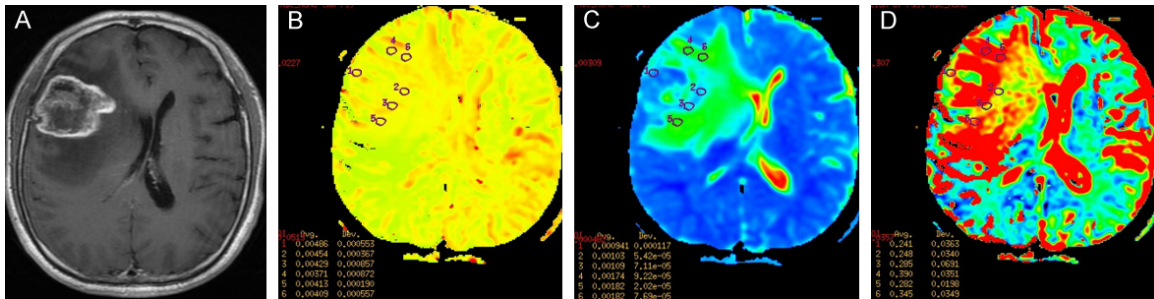


Figure 1. Intravoxel incoherent motion imaging of glioblastoma (WHO grade IV, IDH-wild type). A. Glioblastoma, centered in the right frontal lobe, as seen on axial, contrast-enhanced, T1-weighted imaging. B. IVIM-derived D^* showed increased perfusion in the corresponding, solid, enhancing lesion of the tumor. C. IVIM-derived D showed the D values of peritumoral edema within 1 cm were higher than tumor parenchyma and contralateral centrum semiovale. D. IVIM-derived f showed the order of f values from large to small was peritumoral edema within 1 cm, tumor parenchyma, and contralateral centrum semiovale.

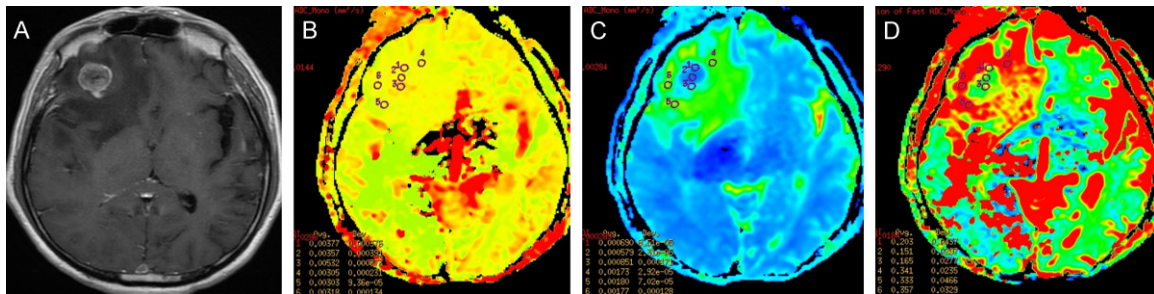


Figure 2. Intravoxel incoherent motion imaging of metastatic tumor (derived from lung, poorly differentiated adenocarcinoma). A. Metastatic tumor, centered in the bottom of right frontal lobe, as seen on axial, contrast-enhanced, T1-weighted imaging. B. IVIM-derived D^* showed increased perfusion in the corresponding, solid, enhancing lesion of the tumor. C. IVIM-derived D showed the D values of peritumoral edema within 1 cm were higher than tumor parenchyma and contralateral centrum semiovale. D. IVIM-derived f showed the order of f values from large to small was peritumoral edema within 1 cm, tumor parenchyma, and contralateral centrum semiovale.

Table 2. Comparison of parameters in peritumoral edema of high-grade gliomas and metastatic tumors

Parameters	High-grade gliomas	Metastatic tumors	t-value	P-value
$D^* (\times 10^{-3} \text{ mm}^2/\text{s})$	4.11±1.19	2.83±6.01	-4.315	<0.001
$rD^* (\times 100\%)$	1.67±0.57	1.25±0.64	-2.154	0.038
$D (\times 10^{-4} \text{ mm}^2/\text{s})$	13.27±3.28	12.65±2.69	-0.653	0.518
$rD (\times 100\%)$	2.03±0.57	1.96±0.46	-0.418	0.678
$f (\%)$	26.60±5.82	36.02±11.37	3.173	0.003
$rf (\times 100\%)$	1.86±0.50	2.50±0.71	3.206	0.003

Data were showed as mean ± SD.

capillary perfusion of high-grade gliomas is higher than that of metastatic tumors, probably resulted from the different growth pattern. Researches in pathology [4, 5] show that high-grade gliomas develop in an invasive manner. They can produce large amounts of neoangiogenesis which are morphologically twisted, structurally immature, and high permeability. The degree and range of vascular proliferation

in metastatic tumors are lower than that of high-grade gliomas. Therefore, high-grade gliomas have a higher rate of capillary perfusion than metastatic tumors, but some researchers [6] have suggested a conclusion contrary to our findings, they believed that the differences in capillary perfusion between high-grade gliomas and metastatic tumors are not statistically significant. PWI, DCE-MRI, ASL and IVIM-DWI performed based on different principles may produce slightly different results. The uniformity of different magnetic resonance imaging techniques needs further study.

This study found that D^* values obtained from peritumoral edema within 1 cm of high-grade gliomas (4.11±1.19) were higher than meta-

Differentiation of high-grade gliomas and brain metastases by IVIM-DWI

Table 3. The values of AUC, sensitivity, specificity and suggested threshold values for D^* , rD^* , f , rf from the ROC curve

Parameters	AUC	P-value	Sensitivity (%)	Specificity (%)	Threshold value
D^* in tumor parenchyma ($\times 10^{-3}$ mm ² /s)	0.733	0.013	94.4	47.6	4.21
rD^* in tumor parenchyma ($\times 100\%$)	0.709	0.026	77.8	61.9	1.66
f in tumor parenchyma (%)	0.765	0.005	66.7	83.3	0.222
rf in tumor parenchyma ($\times 100\%$)	0.815	0.001	81.0	77.8	1.45
D^* in peritumoral edema ($\times 10^{-3}$ mm ² /s)	0.910	<0.001	100	76.2	3.19
rD^* in peritumoral edema ($\times 100\%$)	0.751	0.007	88.9	66.7	1.17
f in peritumoral edema (%)	0.733	0.013	38.1	100	0.357
rf in peritumoral edema ($\times 100\%$)	0.772	0.004	71.4	72.2	2.06

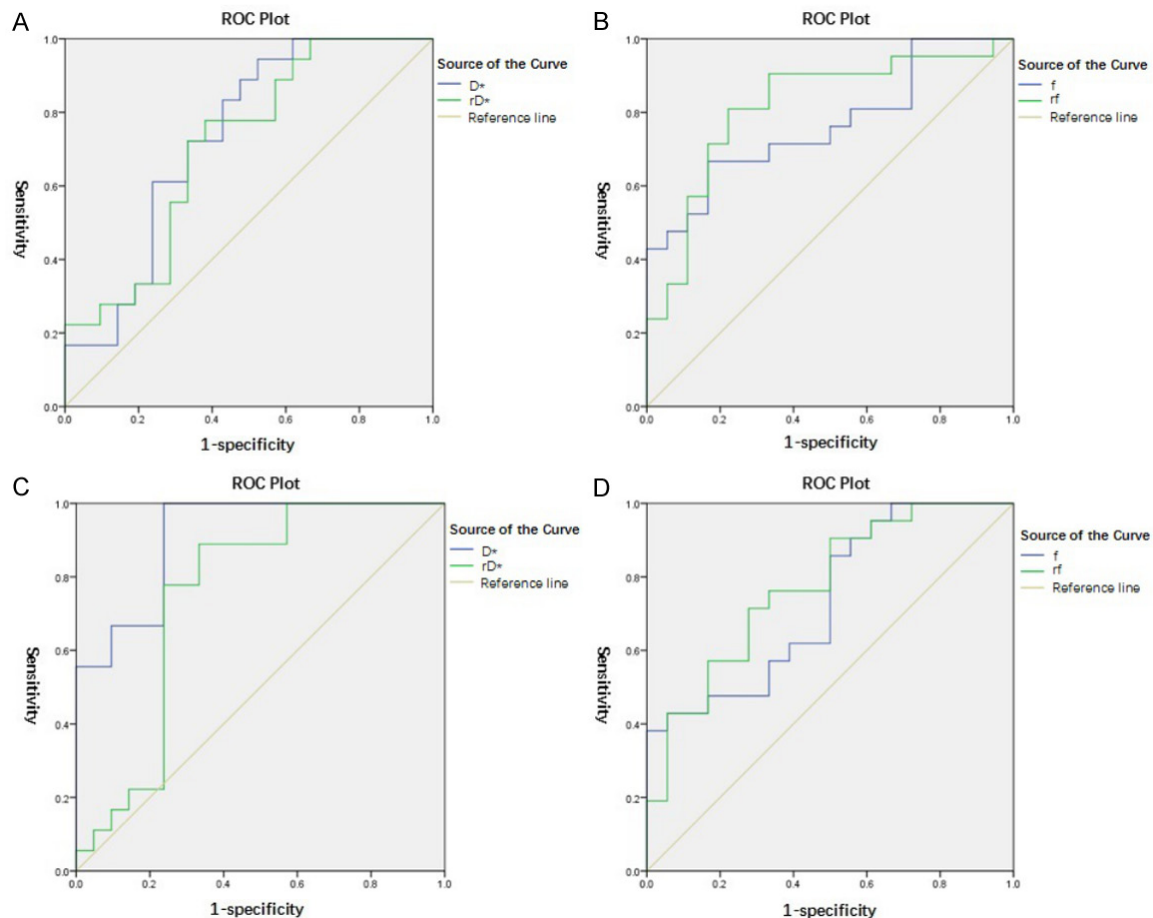


Figure 3. ROC curves according to D^* , rD^* , f , and rf in tumor parenchyma and peritumoral edema within 1 cm. A. Performance differences of D^* , rD^* values in tumor areas in high-grade gliomas and metastatic tumors; B. Performance differences of f , rf values in tumor areas in high-grade gliomas and metastatic tumors; C. Performance differences of D^* , rD^* values in peritumoral edema within 1 cm in high-grade gliomas and metastatic tumors; D. Performance differences of f , rf values in peritumoral edema within 1 cm in high-grade gliomas and metastatic tumors.

static tumors (2.83 ± 6.01), with statistical significance ($P < 0.001$), which may be attributed to the different pathological changes and mechanisms of the edema of the tumors. High-

grade gliomas develop in an invasive manner, where tumor cells can infiltrate normal brain tissue along nerve bundles and inter-vessel space, resulting in the presence of tumor cells

Differentiation of high-grade gliomas and brain metastases by IVIM-DWI

in edema regions surrounding tumors [7]. Peritumoral edema of metastatic tumors is vasogenic edema caused by multiple factors, and no tumor cells infiltrate in the edema area, there is no neoangiogenesis around metastatic tumors either, so peritumoral edema of metastatic tumors has a lower perfusion than high-grade gliomas.

This study also found that D values in peritumoral edema within 1 cm of metastatic tumors were not statistically different between high-grade gliomas and metastatic tumors, differing from our expectations. High-grade gliomas are invasive tumors, and tumor cells can often be found in the edema area surrounding the tumors, as opposed to metastatic tumors whose edema are a simple vasogenic edema. Analyzing the reasons for this statistical result, we proposed several possibilities: 1) Infiltration of tumor cells in high-grade gliomas causes increased cellular density of peritumoral edema within 1 cm, causing diffusion of water molecules to be limited. But infiltration of tumor cells destroys the normal brain structure of peritumoral edema within 1 cm, widening of the inter-cellular spaces between normal cells and causing increased water molecule diffusion; 2) The growth speed of metastatic tumors is faster than high-grade gliomas, resulting compression effect in the surrounding normal brain parenchyma, and forming a relatively “dense band” to decrease inter-cellular space [8, 9], then limiting water molecule diffusion. But vasogenic edema may lead to an increase of water molecules in inter-cellular space, water molecule may move faster relatively. A combination of the above possibilities may account for the lack of statistical significance in the D values obtained in peritumoral edema within 1 cm between high-grade gliomas and metastatic tumors.

It is noteworthy that D^* and f values are both parameters about perfusion, and they should have relevance or consistency in theory [10, 11]. f values should increase with the increasing of microscopic circulation perfusion, but our results seem opposite to the theory. We found the f values of peritumoral edema within 1 cm were higher than tumor parenchyma and contralateral centrum semiovale. These “contradictions” have appeared in other studies [12-15]. f values are closely linked to TE, the longer

the TE, the more obvious attenuation will be at low b-values. In other words, the larger the f value is, especially in tissues where T2 is far lower than the corresponding T2 in blood, the more obvious the dependence of the f values on TE is. When calculating the f value, the effects of differences in T2 cannot be ignored. It should be adjusted. Therefore, the f values obtained in this study may not be the true values. At present, there are no existing reports of “real f values”, it awaits future study.

This set of results showed that AUC values of D^* , rD^* , f , and rf values from the tumor parenchyma and peritumoral edema within 1 cm were both larger than 0.7, reflecting some reference value for tumor identification.

Recently, IVIM-DWI has been more used in liver, breast, and prostate tumors and so on [16-20]. Its applications in head tumors have mainly focused on the preoperative histological grading of gliomas [11, 12]. There are few applications in the differential diagnosis of brain tumors [21-23]. In our study, there are many limitations as follow: ① In ROI selection, the internal signal of the tumor was not uniform in some cases. Even though 3 ROIs were selected and values were averaged, pathology and imaging could not be compared directly. Therefore, selecting a completely accurate pathological section in imaging remains challenging. In addition, as manually measured data in this study, subjectivity led to a measurement error to certain degree. ② Another limitation of this study is that we did not measure T2 values of tissues, which led to T2 correction could not be performed, as a result, the f values obtained in the study may less creditable. ③ At present, optimal b values in IVIM-DWI have yet to be standardized, thus there are still differences in research results. Large-scale, multi-centre pre-clinical studies should be completed to improve parameter setups, and establish a consensus in the field.

In conclusion, parameters based on IVIM-DWI revealed the fast diffusion process of capillary perfusion and the slow diffusion process of water molecules separately and non-invasively. Therefore, the IVIM model can potentially provide more accurate information of tumor diffusion and perfusion characteristics. It has important application values in the differential

diagnosis of high-grade gliomas and metastatic tumors.

Disclosure of conflict of interest

None.

Address correspondence to: Shuangshuang Song and Lei Niu, Department of Radiology, The Affiliated Hospital of Qingdao University, Qingdao, China. Tel: 0086-13220866966; E-mail: song2222shuang@163.com (SSS); Tel: 0086-18661805073; E-mail: hera007@sina.com (NL)

References

- [1] Le Bihan D. Intravoxel incoherent motion imaging using steady-state free precession. *Magn Reson Med* 1988; 7: 346-351.
- [2] Le Bihan D. Magnetic resonance imaging of perfusion. *Magn Reson Med* 1990; 14: 283-292.
- [3] Li JR, Nguyen HT, Nguyen DV, Haddar H, Coatléven J, Le Bihan D. Numerical study of a macroscopic finite pulse model of the diffusion MRI signal. *J Magn Reson* 2014; 248: 54-65.
- [4] Wesseling P, Ruiters DJ, Burger PC. Angiogenesis in brain tumors; pathobiological and clinical aspects. *Neurooncol* 1997; 32: 253-265.
- [5] Nakai T, Muraki S, Bagarinao E, Miki Y, Takehara Y, Matsuo K, Kato C, Sakahara H, Isoda H. Application of independent component analysis to magnetic resonance imaging for enhancing the contrast of gray and white matter. *Neuroimage* 2004; 21: 251-260.
- [6] Tsougos I, Svolos P, Kousi E, Fountas K, Theodorou K, Fezoulidis I, Kapsalaki E. Differentiation of glioblastoma multiforme from metastatic brain tumor using proton magnetic resonance spectroscopy, diffusion and perfusion metrics at 3 T. *Cancer Imaging* 2012; 12: 423.
- [7] Blasel S, Jurcoane A, Franz K, Morawe G, Pelikan S, Hattingen E. Elevated peritumoral rCBV values as a mean to differentiate metastases from high-grade gliomas. *Acta Neurochir (Wien)* 2010; 152: 1893-1899.
- [8] Stadnik TW, Chaskis C, Michotte A, Shabana WM, van Rompaey K, Luypaert R, Budinsky L, Jellus V, Osteaux M. Diffusion-weighted MR imaging of intracerebral masses: comparison with conventional MR imaging and histologic findings. *AJNR Am J Neuroradiol* 2001; 22: 969-976.
- [9] Schaefer PW, Grant PE, Gonzalez RG. Diffusion-weighted MR imaging of the brain. *Radiology* 2000; 217: 331-345.
- [10] Bisdas S, Koh TS, Roder C, Braun C, Schittenhelm J, Ernemann U, Klose U. Intravoxel incoherent motion diffusion-weighted MR imaging of gliomas: feasibility of the method and initial results. *Neuroradiology* 2013; 55: 1189-1196.
- [11] Osamu Togao, Akio Hiwatashi, Koji Yamashita, Kazufumi Kikuchi, Masahiro Mizoguchi, Koji Yoshimoto, Satoshi O. Suzuki, Toru Iwaki, Makoto Obara, Marc Van Cauteren, Hiroshi Honda. Differentiation of high-grade and low-grade diffuse gliomas by intravoxel incoherent motion MR imaging. *Neuro Oncol* 2016; 18: 132-141.
- [12] Hu YC, Yan LF, Wu L, Du P, Chen BY, Wang L, Wang SM, Han Y, Tian Q, Yu Y, Xu TY, Wang W, Cui GB. Intravoxel incoherent motion diffusion-weighted MR imaging of gliomas: efficacy in preoperative grading. *Sci Rep* 2014; 4: 7208.
- [13] Zhang SX, Jia QJ, Zhang ZP, Liang CH, Chen WB, Qiu QH, Li H. Intravoxel incoherent motion MRI: emerging applications for nasopharyngeal carcinoma at the primary site. *Eur Radiol* 2014; 24: 1998-2004.
- [14] Lewin M, Fartoux L, Vignaud A, Arrivé L, Menu Y, Rosmorduc O. The diffusion-weighted imaging perfusion fraction f is a potential marker of sorafenib treatment in advanced hepatocellular carcinoma: a pilot study. *Eur Radiol* 2011; 21: 281-290.
- [15] Lemke A, Laun FB, Simon D, Stieltjes B, Schad LR. An in vivo verification of the intravoxel incoherent motion effect in diffusion-weighted imaging of the abdomen. *Magn Reson Med* 2010; 64: 1580-1585.
- [16] Zhu L, Zhu L, Shi H, Wang H, Yan J, Liu B, Chen W, He J, Zhou Z, Yang X, Liu T. Evaluating early response of cervical cancer under concurrent chemo-radiotherapy by intravoxel incoherent motion MR imaging. *BMC Cancer* 2016; 16: 79.
- [17] Ganten MK, Schuessler M, Bäuerle T, Muentner M, Schlemmer HP, Jensen A, Brand K, Dueck M, Dinkel J, Kopp-Schneider A, Fritzsche K, Stieltjes B. The role of perfusion effects in monitoring of chemoradiotherapy of rectal carcinoma using diffusion-weighted imaging. *Cancer Imaging* 2013; 13: 548.
- [18] Liu C, Liang C, Liu Z, Zhang S, Huang B. Intravoxel incoherent motion (IVIM) in evaluation of breast lesions: comparison with conventional DWI. *Eur J Radiol* 2013; 82: e782-e789.
- [19] Chow AM, Gao DS, Fan SJ, Qiao Z, Lee FY, Yang J, Man K, Wu EX. Liver fibrosis: an intravoxel incoherent motion (IVIM) study. *J Magn Reson Imaging* 2012; 36: 159-167.
- [20] Zhang YD, Wang Q, Wu CJ, Wang XN, Zhang J, Liu H, Liu XS, Shi HB. The histogram analysis of diffusion-weighted intravoxel incoherent motion (IVIM) imaging for differentiating the gleason grade of prostate cancer. *Eur Radiol* 2015; 25: 994-1004.

Differentiation of high-grade gliomas and brain metastases by IVIM-DWI

- [21] Suh CH, Kim HS, Lee SS, Kim N, Yoon HM, Choi CG, Kim SJ. Atypical imaging features of primary central nervous system lymphoma that mimics glioblastoma: utility of intravoxel incoherent motion MR imaging. *Radiology* 2014; 272: 504-513.
- [22] Federau C, O'Brien K, Meuli R, Hagmann P, Maeder P. Measuring brain perfusion with intravoxel incoherent motion (IVIM): initial clinical experience. *J Magn Reson Imaging* 2014; 39: 624-632.
- [23] Maeda M, Kawamura Y, Tamagawa Y, Matsuda T, Itoh S, Kimura H, Iwasaki T, Hayashi N, Yamamoto K, Ishii Y. Intravoxel incoherent motion (IVIM) MRI in intracranial, extraaxial tumors and cysts. *J Comput Assist Tomogr* 1992; 16: 514-518.